NOVI SAD J. MATH
VOL. 28, NO. 3, 1998, 71-93

ON THE ANALYTICAL AND NUMERICAL TREATMENT OF A CLASS OF PDE'S WITH THE APPLICATION TO SOME TWO-VALLEY SEMICONDUCTOR ELECTRON DEVICES

Bratislav D. Iričanin, Goran Z. Mašanović, Dejan M. Gvozdić
University of Belgrade, Faculty of Electrical Engineering
Bulevar revolucije 73, P. O. Box 35-54, 11120 Belgrade, YU-Serbia
E-mail: iricanin@buef31.etf.bg.ac.yu

Abstract

The system of linear partial differential equations (PDE) of the first order, with initial conditions given by the HEAVISIDE (step) function, is considered. It is shown that the system can be solved analytically (in the terms of integrals), where the problem of numerical quadratures arises. Some integrals are improper (singular in the upper bound), but considering their convergence and calculating their principal value (in a CAUCHY sense), the problem can be successfully solved. In the special case the achieved results have been significantly simplified and then compared with the numerical solution obtain-ed by the application of the finite differences method, namely the up-wind scheme, which is used most often for that kind of problems. A detailed analysis of the obtained error, with some graphical illustrations for various values of parameters, is given. The proposed initial value problem has several applications, e.g., in semiconductor physics, where it is a good model for the inter-valley transfer in a two-valley semiconductor electron devices in the case when the electric field is stationary and homogeneous.

AMS Mathematics Subject Classification (1991): primary 35E15, secondary 82C23, 35L70, 58G16, 35C05.
Computing Reviews Classification Scheme (1992): Primary J.2, Secondary I.6
PACS numbers: 72.10.-d, 72.10.Bg
Keywords and Phrases: system of PDEs, PDE of hyperbolic type, two-valley semiconductor, inter-valley transfer.

1. Introduction

Starting from a system of the first order partial differential equation (PDE) , we intend to obtain that particular solution (in an analytically closed form) which satisfies the specifically established initial conditions. The observed PDE system with the relative-ly general type of initial conditions can be a good mathematical model for various kinds of problems. In the application we will consider some physical problems, namely the modelling of some microelectronic devices operation that hitherto has not been considered in this exact way.

2. The model

Let us consider the following set of PDEs with respect to the spatial-temporal n_1 and n_2 distribution:

$$\begin{aligned} \frac{\partial n_1}{\partial t} + v_1 \frac{\partial n_1}{\partial x} &= -\frac{n_1}{\tau_1} + \frac{n_2}{\tau_2} + G, \\ \frac{\partial n_2}{\partial t} + v_2 \frac{\partial n_2}{\partial x} &= -\frac{n_2}{\tau_2} + \frac{n_1}{\tau_1}, \end{aligned} \tag{1}$$

where x and t are the independent variables. The multiplying factors v_1 and v_2, as well as τ_1 and τ_2, are constant with respect to the independent variables.

In order to solve the PDE system (1) it is necessary to define initial and / or boundary conditions. Let us assume that:

$$\begin{aligned} n_1(x,0) &= Cf(x)\,\mathrm{h}(x), \\ n_2(x,0) &= 0, \end{aligned} \tag{2}$$

where $f:[0,d]\to\mathbf{R}$ is an arbitrary function differentiable on the segment $[0,d]$, $\mathrm{h}(x)$ denotes the HEAVISIDE (step) function, and C is a constant. There is a physical reason for defying DIRICHLET-type boundary conditions at its boundaries using $\mathrm{h}(x)$. Finally, assume that the addend G in the first equation is

$$G = Cf(x)\,\mathrm{h}(x)\delta(t), \tag{3}$$

where $\delta(t)$ is the DIRAC delta function[1]. The relations (2) are obtained by integration of system (1) from $t=0^-$ to $t=0^+$, taking into account only relations (3).

---

[1] Here, as well as in the further text, we use that (customary) name, although it would be more appropriate to use the phrase "the DIRAC *delta distribution*".

3. Analytical treatment

The problem to be solved (1)-(2) can be recognized as the CAUCHY problem. For that purpose, the initial conditions are directly expanded in the following manner:

$$n_1(x,0) = Cf(x)\,\mathrm{h}(x),$$

(4a)
$$\frac{\partial n_1(x,0)}{\partial t} = -C\left(\left(\frac{f(x)}{\tau_1} + v_1 f'(x)\right)\mathrm{h}(x) + v_1 f(x)\delta(x)\right);$$

$$n_2(x,0) = 0,$$

(4b)
$$\frac{\partial n_2(x,0)}{\partial t} = \frac{C}{\tau_1} f(x)\,\mathrm{h}(x).$$

Let us try to transform the problem under consideration into a form more convenient for solving. We shall transform the system of PDE into the equation of second order with respect to n_1, (i = 1, 2). By removing the dependent variable n_2 from the system (1) we reduce it to the desirable second-order PDE over n_1:

$$\frac{\partial^2 n_1}{\partial t^2} + (v_1 + v_2)\frac{\partial^2 n_1}{\partial x \partial t} + v_1 v_2 \frac{\partial^2 n_1}{\partial x^2} + \left(\frac{v_1}{\tau_2} + \frac{v_2}{\tau_1}\right)\frac{\partial n_1}{\partial x} + \left(\frac{1}{\tau_1} + \frac{1}{\tau_2}\right)\frac{\partial n_1}{\partial t} = 0.$$

(5)

By introducing new independent variables α and β via the transformation

(6)
$$\alpha = x - \frac{t}{2}(v_1 + v_2),\quad \beta = \frac{t}{2}(v_2 - v_1)$$

and by replacing n_1 by a new dependent variable w according to

(7)
$$n_1 = \mathrm{e}^{-(A+B)\alpha + (A-B)\beta}\, w(\alpha,\beta),$$

where

(8)
$$A = \frac{1}{\tau_1(v_1 - v_2)};\quad B = -\frac{1}{\tau_2(v_1 - v_2)},$$

the equation (5) assumes the following form:

(9)
$$\frac{\partial^2 w}{\partial \alpha^2} - \frac{\partial^2 w}{\partial \beta^2} + \frac{4}{\sqrt{\tau_1 \tau_2}\,|v_1 - v_2|} w = 0.$$

The expanded initial conditions (4a) become

$$w_0(\alpha) = w(\alpha,0) = C\,\mathrm{e}^{(A+B)\alpha} f(\alpha)\,\mathrm{h}(\alpha) = \psi_0^{(1)}(\alpha)\,\mathrm{h}(\alpha),$$

$$w_1(\alpha) = \frac{\partial w(\alpha,0)}{\partial \beta} = C\,\mathrm{e}^{(A+B)\alpha}\left(\left((A+B)f(\alpha) + \frac{2}{1-\nu_2/\nu_1} f'(\alpha)\right)\mathrm{h}(\alpha) + \right.$$

$$\left. + \frac{2}{1-\nu_2/\nu_1} f(\alpha)\delta(\alpha)\right) = \psi_1^{(1)}(\alpha)\,\mathrm{h}(\alpha) + \psi_2^{(1)}(\alpha)\delta(\alpha).$$

(10)

The obtained problem (9)-(10) is more convenient for solving than the initial problem (1)-(4). Equation (10) can be recognized as a *hyperbolic type* PDE with a self-ad-joint inherent operator. The obtained equation is a special case of the so-called gene-ral *telegraphic equation* whose special cases are described in [2, 6, 17]. It is solved by using the RIEMANN method. It can be achieved that the RIEMANN function V is

$$V = \mathrm{J}_0\left(\frac{2}{\sqrt{\tau_1\tau_2}\,|\nu_1-\nu_2|}\sqrt{(x-\nu_1 t)(x-\nu_2 t)}\right), \tag{11}$$

where $\mathrm{J}_n(x)$ denotes a BESSEL function of the first kind of the n^{th} order. For the so-lution of the PDE (9) with the initial conditions (10) we obtain:

$$w(\alpha-\beta,\alpha+\beta) = \frac{1}{2}\left(w_0(\alpha-\beta) + w_0(\alpha+\beta)\right) +$$

$$+\frac{1}{2}\int_{\alpha-\beta}^{\alpha+\beta} \mathrm{J}_0\left(\frac{2}{\sqrt{\tau_1\tau_2}\,|\nu_1-\nu_2|}\sqrt{(\alpha-\beta-\xi)(\alpha+\beta-\xi)}\right) w_1(\xi)\,\mathrm{d}\xi -$$

$$-\frac{t}{2\tau_1\tau_2|\nu_1-\nu_2|}\int_{\alpha-\beta}^{\alpha+\beta} \mathrm{J}_1\left(\frac{2}{\sqrt{\tau_1\tau_2}\,|\nu_1-\nu_2|}\sqrt{(\alpha-\beta-\xi)(\alpha+\beta-\xi)}\right) w_0(\xi)\,\mathrm{d}\xi. \tag{12}$$

Let us introduce a new variable θ:

$$\theta = 2\sqrt{\frac{-1}{\tau_1\tau_2(\nu_1-\nu_2)^2}(\alpha+\beta-\xi)(\alpha-\beta-\xi)}. \tag{13}$$

It stems from here that

$$\xi = \xi_j(\theta) = \alpha + \frac{(-1)^j}{2}\sqrt{\tau_1\tau_2}\,|\nu_1-\nu_2|\sqrt{\left(\frac{t}{\sqrt{\tau_1\tau_2}}\right)^2 - \theta^2}, \tag{14}$$

where for $\alpha \geq \xi$ is $j = 1$, while $\alpha < \xi$ implies $j = 2$. From (13) it can be seen that $\theta \in \left[0, \frac{t}{\sqrt{\tau_1 \tau_2}}\right]$ 1, while for the variables ξ_j the following limitations are valid: $\xi_1 \in \left[x - v_1 t, x - \frac{v_1 + v_2}{2} t\right]$ and $\xi_2 \in \left[x - \frac{v_1 + v_2}{2} t, x - v_2 t\right]$. 2 Now we transform the obtained solution (12) to enable its use for the starting problem. Also, we utilize the relation $I_n(z) = (-i)^n J_n(iz)$, where $I_n(x)$ is the modified BESSEL function of the first kind and n^{th} order, valid for all complex values $z \in C$.

Now we analyze the HEAVISIDE factors in the integrand functions of the solution implicitly involved in (12). Depending on their non-zero values, the solution (spatial-temporal dependence) can be split into four parts (not forgetting that x and t cannot be negative). In the first region $x > v_1 t$ 3is valid; here the values of the HEAVISIDE functions are $h(\xi_1(\theta)) = h(\xi_2(\theta)) = 1.4$ The second region is described by the inequalities $\frac{v_1 + v_2}{2} t < x \leq v_1 t$ 5 and in it is $h(\xi_1(\theta)) = \begin{cases} 1, & \theta > \theta_C \\ 0, & \theta < \theta_C \end{cases}$, while $h(\xi_2(\theta)) = 1$ 6 (in the whole region). The third region is characterized by the relation $v_2 t < x \leq \frac{v_1 + v_2}{2} t$ 7, and there is $h(\xi_2(\theta)) = \begin{cases} 1, \theta < \theta_C \\ 0, \theta > \theta_C \end{cases}$ and $h(\xi_1(\theta)) = 0$ (in the whole region). In the remaining - fourth - region is $x \leq v_2 t$ and the values of the HEAVISIDE functions are $h(\xi_1(\theta)) = h(\xi_2(\theta)) = 0$. In our previous consideration we have introduced a cutoff value θ_C of the variable θ, equal to

$$\theta_C = \frac{2}{\sqrt{\tau_1 \tau_2}\,|v_1 - v_2|} \sqrt{(v_1 t - x)(x - v_2 t)}. \tag{15}$$

In formula (12) only those addends remain for which $h(\xi_i(\theta)) = 1$, $(i = 1, 2)$, is valid. This suggests that the solution itself can be separated into four different expressions valid in particular regions which are shown in Figure 1.

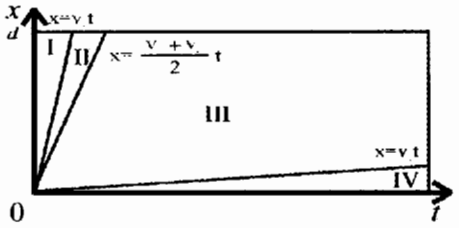

Figure 1 Regions (I-IV) in the spatial-temporal dependence.

Using the property of the DIRAC δ function

$$\int_a^b \delta(x)\mathrm{d}x = \begin{cases} 0, & 0 \notin [a,b], \\ 1, & 0 \in [a,b] \end{cases} \tag{16}$$

which stems directly from its definition, we conclude that the result of the integration of the part of integrand including $\delta(\xi_1(\theta))$ or $\delta(\xi_2(\theta))$ depends only on whether the functions $\xi_1(\theta)$ and $\xi_2(\theta)$ reach zero value in the segment $\theta \in \left[0, \frac{t}{\sqrt{\tau_1 \tau_2}}\right]$ 8, for the considered values of the variable x. If these function are not equal to zero within this segment, the integral of this part of the integrand will be equal to zero. This is just what happens in the regions I and IV. In the regions II and III the functions $\xi_1(\theta)$ and $\xi_2(\theta)$ change their signs, as established by the previous analysis of HEAVISIDE func-tions, so that in these regions the integrals are non-zero.

Finally, by an approriate rearrangement of the addends in the integrated expression, the obtained solution is reduced to the following formulae:

- for $x > v_1 t$:

(17a)

$$w(x,t) = \frac{1}{2}\left(\psi_0^{(1)}(x - v_1 t) + \psi_0^{(1)}(x - v_2 t)\right) + F_1\left(0, \frac{t}{\sqrt{\tau_1 \tau_2}}\right) + F_2\left(0, \frac{t}{\sqrt{\tau_1 \tau_2}}\right);$$

- for $v_1 t \geq x > \frac{t}{2}(v_1 + v_2)$:

$$(17b)\quad w(x,t) = \frac{1}{2}\psi_0^{(1)}(x - v_2 t) + F_1\left(\theta_C, \frac{t}{\sqrt{\tau_1 \tau_2}}\right) - D(\theta_C, t) + F_2\left(0, \frac{t}{\sqrt{\tau_1 \tau_2}}\right);$$

- for $\frac{t}{2}(v_1 + v_2) \geq x > v_2 t$:

(17c) $$w(x,t) = \frac{1}{2}\psi_0^{(1)}(x - v_2 t) + F_2(0,\theta_C) - D(\theta_C,t);$$

- for $v_2 t \geq x \geq 0$:

(17d) $$w(x,t) = 0,$$

that will be additionally elucidated. We define the functions $F_i(a,b)$ as integrals given by the following expressions:

(18) $$F_i(a\,b) = \int_a^b \frac{p_{fi}(\theta)\,\mathrm{d}\theta}{\sqrt{\left(\frac{t}{\sqrt{\tau_1\tau_2}}\right)^2 - \theta^2}},$$

where

(19)

$$p_{fi}(\theta) = -\frac{\sqrt{\tau_1\tau_2}\,|v_1 - v_2|}{4}\theta I_0(\theta)\psi_1^{(1)}(\xi_i(\theta)) + \frac{t}{2\sqrt{\tau_1\tau_2}} I_1(\theta)\psi_0^{(1)}(\xi_i(\theta)).$$

Let us remember that the functions $\psi_0^{(1)}$ 9 and $\psi_1^{(1)}$ 10 are defined in the transformed expanded initial conditions (10). The functions $F_i(a, b)$ have been introduced to make the expression of the solution (17a-d) less comprehensive, but they are also algorithm-ically convenient from the aspect of software implementation.

Consequently, from the nature of initial conditions, namely the part of the inte-grand comprising the DIRAC delta functions $\delta(\xi_1(\theta))$ and $\delta(\xi_2(\theta))$, the addend $D(\theta_{C,,}, t)$ in (17b-c) is:

(20) $$D(\theta_C,t) = \frac{C v_1 \sqrt{\tau_1\tau_2}}{2} \frac{\theta_C I_0(\theta_C) f(0)}{\sqrt{\left(\frac{t}{\sqrt{\tau_1\tau_2}}\right)^2 - \theta_C{}^2}}.$$

In the expression (18) we calculate the principal value of the integral (v. p. in CAUCHY sense) in the case of a singularity in the upper boundary.

Finally,

(21) $$n_1(x,t) = \mathrm{e}^{k_x x + k_t t} w(x,t),$$

where the exponential coefficients are

$$k_x = \frac{\tau_1 - \tau_2}{\tau_1 \tau_2 (v_1 - v_2)}; \quad k_t = \frac{v_2 \tau_2 - v_1 \tau_1}{\tau_1 \tau_2 (v_1 - v_2)}, \tag{22}$$

which originated from expressions (6)-(8).

The solution for the function n_2 can be obtained by an analogous procedure, bearing in mind that the starting system is reduced to the same equation (9). The difference is that the expanded initial conditions (4b) are in this case

$$w_0(\alpha) = w(\alpha,0) = 0,$$

$$w_1(\alpha) = \frac{\partial w(\alpha,0)}{\partial \beta} = -2CA\, \mathrm{e}^{(A+B)\alpha} f(\alpha) \mathrm{h}(\alpha) = \psi_1^{(2)}(\alpha) \mathrm{h}(\alpha). \tag{23}$$

The following formulae are obtained:

- for $x > v_1 t$:

$$n_2(x,t) = \mathrm{e}^{k_x x + k_t t} \left(H_1\left(0, \frac{t}{\sqrt{\tau_1 \tau_2}}\right) + H_2\left(0, \frac{t}{\sqrt{\tau_1 \tau_2}}\right)\right); \tag{24a}$$

- for $v_1 t \geq x > \frac{t}{2}(v_1 + v_2)$:

$$n_2(x,t) = \mathrm{e}^{k_x x + k_t t} \left(H_1\left(\theta_C, \frac{t}{\sqrt{\tau_1 \tau_2}}\right) + H_2\left(0, \frac{t}{\sqrt{\tau_1 \tau_2}}\right)\right); \tag{24b}$$

- for $\frac{t}{2}(v_1 + v_2) \geq x > v_2 t$:

$$n_2(x,t) = \mathrm{e}^{k_x x + k_t t} H_2(0, \theta_C); \tag{24c}$$

- for $v_2 t \geq x \geq 0$:

$$n_2(x,t) = 0. \tag{24d}$$

The integrals $H_i(a,b)$ are defined in the following manner:

$$H_i(a,b) = -\frac{\sqrt{\tau_1 \tau_2}\,|v_1 - v_2|}{4} \int_a^b \frac{p_{\mathrm{hi}}(\theta)\, \mathrm{d}\theta}{\sqrt{\left(\frac{t}{\sqrt{\tau_1 \tau_2}}\right)^2 - \theta^2}}, \tag{25}$$

with the well-behaved part of the integrand function equal to

(26) $$p_{\mathrm{hi}}(\theta) = \theta \mathrm{I}_0(\theta)\, \psi_1^{(2)}(\xi_i(\theta)).$$

In this manner we practically conclude the analytic solution procedure, where the obtained solutions for $n_1(x, t)$ and $n_2(x, t)$ are continuous functions.

However, let us note that some of the integrals in (18) and (25) are improper. Their form is

(27) $$P(a,b) = \int_a^b \frac{p(\theta)\,\mathrm{d}\theta}{\sqrt{c^2 - \theta^2}},$$

($b \le c$), and it can be seen that for $c = b$ they are singular in the upper boundary. This singularity has the form of an inverse square root. Therefore, the singularity is re-movable. One can obtain

(28) $$P(a,b) = 2 \int_0^{\sqrt{b-a}} \frac{p(b - \vartheta^2)\,\mathrm{d}\vartheta}{\sqrt{2b - \vartheta^2}}.$$

Now we can calculate the obtained integrals by some of the standard methods of numerical integration, taking care about the nature of the integrand function.

Let us note that in the analytical solution (for which it is said to be solved in quadratures) there is nevertheless a part which should be calculated approximately, and this part is the value of the integral. However, bearing in mind the complexity (the order) of the required approximate methods and knowing which integrals and initial equations we are dealing with, we conclude that the proposed methods offer an essential improvement in comparison with the methods utilized up to date in the analysis of the phenomena under consideration by approximate solution of some special cases of the CAUCHY problem (1)-(4).

4. An example of a semiconductor device modelling

The proposed exact treatment of the model described by the PDE system (1) and by the initial conditions of general type (2) or (4) gives results potentially applicable in the modelling of electron transport in semiconductor electron devices. The obtained solution is applied in the special case of electron concentration profile determination in a p-i-n photodiode. A similar treatment is applicable for other semiconductor devices where the mentioned basic assumptions are satisfied (MESFET, HEMT, etc.).

We demonstrate the efficiency of the analytical approach in the example of a p-i-n photodiode with the absorption layer made of a two-valley

semiconductor. This efficiency is reflected not only in the quantitative (numerical) superiority, but also in the possibility of creating a qualitatively clearer and more detailed picture of carrier transport mechanisms in a two-valley semiconductors. Although analytical treatment could be more fruitful than the numerical one, it is not widely applied, not only because one would have to overcome significant difficulties imposed by such a treatment, but also because there is an uncertainty in establishing of presenting solution in an analytically closed form, it is considered in [7]. The advantage in rapidity of reaching the solu-tion (*i.e.*, the number of performed computer operations) is evident, but we did not measure it explicitly, since the numerical processes involved are incomparable [3]. It follows from the fact that the numerical method requires all the previous calculations in the discretization mesh, as opposed to the analytical one. The quality of the analyti-cal solution becomes fully visible in the comparative analysis with approximate solution obtained by purely numerical treatment of the starting equations using the finite difference method.

4.1 Application of the analytical treatment

In the further text we present the analytical solution obtained in Section 3, correspond-ing to the particular case $f(x) \equiv 1$. Under this condition the analytical solution (17a-d) and (24a-d) can be rewritten in a much more compact form that is simpler and more convenient for effective calculations and qualitative consideration. After a number of algebraic transformations (including some integrals from [10]), the expressions for n_1 and n_2 are obtained in the form:

(29)

$$n_1^{(j)}(x,t) = (\delta_{1j} + \delta_{2j}) n_1^{\mathrm{I}}(t) - (\delta_{2j} + \delta_{3j})(-1)^j \left(\frac{C}{2} \mathrm{e}^{-\frac{t}{\tau_{j-1}}} + \mathrm{e}^{k_x x + k_t t} F_{j-1}(0, \theta_{\mathrm{C}}) \right);$$

(30) $n_2^{(j)}(x,t) = (\delta_{1j} + \delta_{2j}) n_2^{\mathrm{I}}(t) - (\delta_{2j} + \delta_{3j})(-1)^j \, \mathrm{e}^{k_x x + k_t t} H_{j-1}(0, \theta_{\mathrm{C}})$,

(j = 1, 2, 3, 4), where the superscript '(j)' corresponds to the particular region shown in Figure 1. In this compact form of the solution δ_{ij} denotes the KRONECKER δ symbol and the 'main' quantities $n_i^{\mathrm{I}}(t)$ are:

(31a) $$n_1^{\mathrm{I}}(t) = C \left(\frac{1}{1 + \tau_2/\tau_1} + \frac{1}{1 + \tau_1/\tau_2} \mathrm{e}^{-t\frac{\tau_1+\tau_2}{\tau_1\tau_2}} \right),$$

(31b) $$n_2^{\mathrm{I}}(t) = \frac{C}{1+\tau_1/\tau_2}\left(1 - \mathrm{e}^{-t\frac{\tau_1+\tau_2}{\tau_1\tau_2}}\right).$$

In establishing the expressions (29) and (30) we have taken into account that the addend (20), stemming from the nature of the initial conditions, has small influence on the obtained concentration values, and can be neglected. It is the consequence of the numerical values of the constants, and, generally speaking, it could not be fulfill-ed. In this special case we have removed all the possibly existing singularities in the integrals (18) and (25).

Regarding the remaining numerical integration (on the interval $(0, \theta_C)$) we have used the ROMBERG method [13], and special care has been granted to the calculation
of the values of modified BESSEL functions (see [9]).

4.2 Numerical treatment

The PDE system (1), or the equivalent PDE (9) (a detailed analysis of such PDEs is given in [16]) is *hyperbolic*. There are various methods that can be applied in numeri-cal calculation of the approximate solution of both the starting and the transformed problem (9)-(10). In our investigation we have decided to use the method of finite differences directly applied to the initial problem (1). Since these equations describe the carrier flow, the choice of the scheme and the discretization steps should be per-formed to accurately describe the transport process in each step. One of the schemes to be found in the literature is the so-called *upwind* scheme [8, 15]. It uses the form of back finite differences and it has shown good results in the treatment of similar phenomena in modelling of two-valley semiconductor devices [5, 11]. Figure 2 shows schematically the mesh-point relevant in each step. The discretization steps over time Δt and position Δx must fulfil the stability criterion which is here given by

(17) $$\Delta x \geq \Delta t \cdot \max_i \{v_i\}.$$

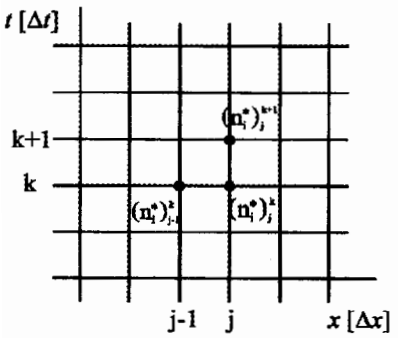

Figure 2 Mesh-point for the upwind scheme for numerical calculation of the PDE system (1) using (33) in terms of $n_i^*(x,t)$, $(i=1,2)$

In the proposed finite difference form, the problem (1)-(4) becomes the following system of difference equations:

$$\frac{(n_1^*)_j^{k+1}-(n_1^*)_j^k}{\Delta t}+\frac{v_1(n_1^*)_j^k-v_1(n_1^*)_{j-1}^k}{\Delta x}=-\frac{(n_1^*)_j^k}{\tau_1}+\frac{(n_2^*)_j^k}{\tau_2},$$
$$\frac{(n_2^*)_j^{k+1}-(n_2^*)_j^k}{\Delta t}+\frac{v_2(n_2^*)_j^k-v_2(n_2^*)_{j-1}^k}{\Delta x}=-\frac{(n_2^*)_j^k}{\tau_2}+\frac{(n_1^*)_j^k}{\tau_1}, \tag{33}$$

with the initial conditions

$$(n_1^*)_j^0=C,\ (n_2^*)_j^0=0, \tag{34a}$$

(for all j), and boundary conditions

$$(n_1^*)_{-1}^k=0,\ (n_2^*)_{-1}^k=0, \tag{34b}$$

(for all k), where the quantities Δt and Δx are chosen conveniently, and $n_i^*=n_i^*(x,t)$, $(i=1,2)$, are numerically obtained solutions for concentrations. In our calculations we have adopted the values $x=0$ $(12.5\cdot10^{-3})$ 5 μm and $t=0$ (10^{-3}) 60 ps, $C=1$. Thus we have obtained the values of the normalized concentration in the conduction band valleys.

4.3 Some notes on the physical background

The electron transport in submicron semiconductor structures is mostly determined by nonstationary effects. The Monte-Carlo simulation has been employed [18] to obtain relatively satisfactory results. Nevertheless, due to the known limitations imposed by the probabilistic approach and its high demands for computer resources, it cannot remain the only method for the analysis of transport processes. Another approach is based on the momentum method from which *the hydrodynamic model* of transport equation is derived [1, 18]. However, this model is very difficult to solve, which is the reason why its approximation – the so-called *phenomenological model* – is used instead [5, 11, 14]. The phenomenological model describes the inter-valley transport in the relaxation time or transfer time approximation, where these times are functions of the electric field [5, 11, 14]. The total electron concentration is determined by the electron concentrations in the central (Γ) valley n_1 and in the satellite (X, L) valleys n_2 of the conduction band. In our further consideration we assume that the electric field is sta-tionary, homogeneous, and strong enough, so that electron diffusion can be neglected. In that case the electron velocity in each of the valleys is determined by the electric field intensity E and electron mobility for the particular valley μ_i:

$$v_i=v_i(E)=\mu_i(E)E,\quad (i=1,2); \tag{35}$$

the index *'1'* corresponds to the central, and *'2'* to the satellite valleys of the con-duction band. The electron velocity in the central valley is larger than in the satellite one ($v_1 > v_2$). Such a situation is encountered in the case of a p-i-n photodiode with absorption layer made of a two-valley semiconductor.

The phenomenological model for electrons is defined by (1). In (2) the "free" addend G denotes generation term for the central valley, the coefficients $\tau_1 = \tau_1(E)$ and $\tau_2 = \tau_2(E)$ are the electron transfer times from the central into the satellite valley (τ_1), and from the satellite into the central one (τ_2) [5, 11, 14]. The segment $[0,d]$ physically represents the space of the semiconductor device under consi-deration, where d is the width of the absorption layer between the p-i-n photodiode contacts. Let us assume that at the initial moment $t = 0$ electrons are generated by optical pulse excitation along the absorption layer only within the central valley (that implies (3)). This situation occurs when the reciprocal value of the absorption coefficient α is much smaller than the absorption layer width ($\alpha^{-1} << d$). In this case the function describing the initial conditions is constant, *i.e.*, $f(x) \equiv 1$.

4.4 The comparative analysis of analytical and numerical solutions with physical consequences

From the obtained relatively simple expressions (29) and (30) it can be observed that there is a general exponential time dependence of concentration. Explicit formulae (29) and (30) point to a certain effect which cannot be observed from the numerically obtained solutions. In those relation there is practically a new time constant describ-ing the concentrations in the valleys of the conduction band. It is equal to the half of harmonic mean of time constants τ_1 and τ_2. In regions I and IV the obtained solution does not depend on the variable x. This is a consequence of the specific initial conditions determined by a constant function f. On the contrary, in the rest of regions (II and III) that dependence exists. Besides, in expressions (29)-(30) (cases i = 2, 3) there is an implicit dependence on v_1 and v_2, which can be seen in formulae (22), (18), (25) and (15). Only the analytical approach shows that within the region where $x > v_1 t$ the following asymptotic relations are valid:

$$n_1 \to \frac{C}{1+\tau_2/\tau_1}, \quad n_2 \to \frac{C}{1+\tau_1/\tau_2}, \tag{36}$$

($t \to \infty$), while generally (in the other regions) the following is valid:

$$n_1 \to 0, \quad n_2 \to 0. \tag{37}$$

However, the relations (36) could be obtained from equation (1), but the restriction for the range of the validity of (36) could not be perceived only from them. Otherwise, relations (36) and (37) describe the saturation process.

We have performed a comparative analysis of our analytical and the standard numeri-cal solution for three representative values of the parameter (electric field intensity E) – for weak (5 kV/cm), intermediate (10 kV/cm) and strong (30 kV/cm) fields activity, when electron "heating" in the semiconductor is intensive.

Figures 3, 6, 9 and 12, 15, 18 are the graphical illustrations of the concentrations n_1 and n_2 (obtained according to Subsection 4.1), respectively, for the characteristic parameter values in a two-valley semiconductor according to [5, 11] (τ_2= 5 ps), as well as for the maximal values of x ($\leq d$ = 5 μm) and t ($\leq$ 60 ps) relevant for this kind of optoelectronic devices. Figures 4, 7, 10 and 13, 16, 19 show the num cal solution coincide for the most part, which is confirmed by Figure 5 representing the spatial-temporal dependence of the difference $\varepsilon_1(x, t)$ between these two results. This difference shows clearly that the largest deviation appears near the straight boundary line $x = v_1 t$ in the regions II and III. It is obvious that the error is largest at the very beginning of the numerical procedure, where the "stepped" boundary condition is posed. From the point of view of the transport processes, this means that the flow of the electrons which did not leave the central valley ($x > v_1 t$) can be successfully described, while the discrepancy occurs for the transport of the electrons returning from the satellite valleys into the central one. The use of a more complex algorithm, for example the "shock-capturing algorithm" (see [4, 12]) can minimize such errors for the cost of increased requirements for processor time and memory storage.
erically obtained concentrations n_1^* and n_2^* (subsection 4.2), respectively, and Figures 5, 8, 11 and 14, 17, 20 depict the values of spatial-temporal distribution of absolute errors $\varepsilon_1 = n_1 - n_1^*$ and $\varepsilon_2 = n_2 - n_2^*$, respectively.

At a first glance it could appear that the solutions shown in Figures 3 and 4 are identical. However, we can see the additional information in the added 2D contour plots. In Figure 3 we can easily see the boundaries of the regions I and IV, *i.e.*, the straight lines $x = v_1 t$ and $x = v_2 t$, while in the numerical solution we can see only the boundary of the region I. Also, it can be seen that for $x > v_1 t$ the analytical and the numerical solution coincide for the most part, which is confirmed by Figure 5 representing the spatial-temporal dependence of the difference $\varepsilon_1(x, t)$ between these two results. This difference shows clearly that the largest deviation appears near the straight boundary line $x = v_1 t$ in the regions II and III. It is obvious that the error is largest at the very beginning of the numerical procedure, where the "stepped" boundary condition is posed.

From the point of view of the transport processes, this means that the flow of the electrons which did not leave the central valley ($x > v_1 t$) can be successfully described, while the discrepancy occurs for the transport of the electrons returning from the satellite valleys into the central one. The use of a more complex algorithm, for example the "shock-capturing algorithm" (see [4, 12]) can minimize such errors for the cost of increased requirements for processor time and memory storage.

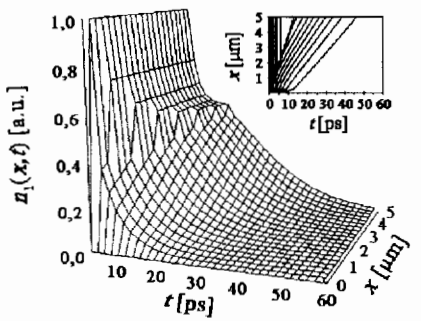

Figure 3 Spatial-temporal distribution of the normalized concentration $n_1(x, t)$ in the central (Γ) valley for the electric field intensity $E = 5$ kV/cm

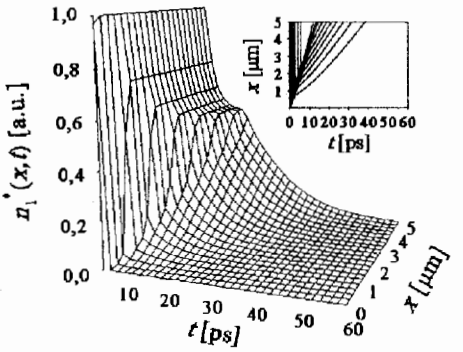

Figure 4 Spatial-temporal distribution of the normalized concentration $n_1^*(x, t)$ in the central (Γ) valley for electric field intensity $E = 5$ kV/cm

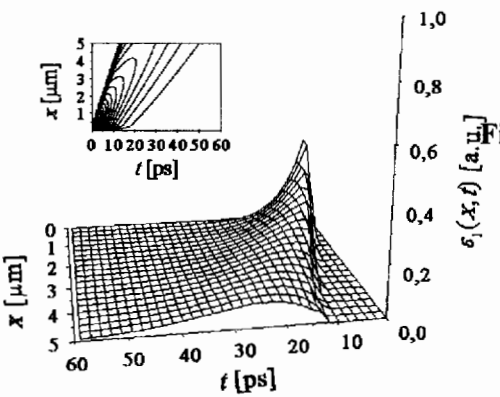

Figure 5 Spatial-temporal distribution of the difference $\varepsilon_1(x, t)$ of the obtained concentrations in the central (Γ) valley for the electric field intensity $E = 5$ kV/cm

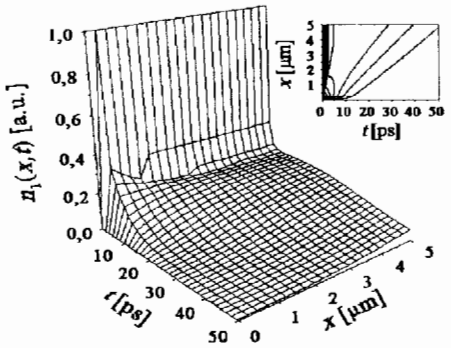

Figure 6. Spatial-temporal distribution of the normalized concentration $n_1(x, t)$ in the central (Γ) valley for the electric field intensity $E = 10$ kV/cm

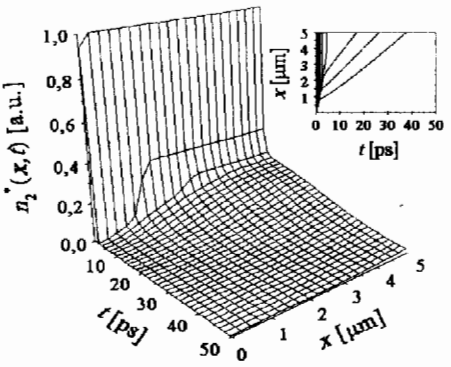

Figure 7 Spatial-temporal distribution of the normalized concentration $n_1^*(x, t)$ in the central (Γ) valley for the electric field intensity E = 10 kV/cm

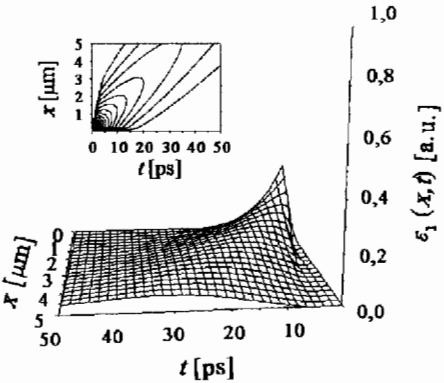

Figure 8 Spatial-temporal distribution of the difference $\varepsilon_1(x, t)$ of the obtained concentrations in the central (Γ) valley for the electric field intensity E=10 kV/cm

With an increase of the intensity of the electric field E the difference in behaviour between the analytical solution (Figures 6 and 9) and numerical one (Figures 7 and 10) for the concentration n_1 becomes more pronounced, although the absolute value of the difference ε_1 decreases (Figures 8 and 11). The decrement of the absolute error is understandable, since due to the intensive inter-valley transfer the values of the func-tions $n_1(x, t)$ and $n_1^*(x, t)$ sharply decrease (toward zero) after the initial moment, which causes the decrease of their difference. However, the observed differences show that, following the strong field activity transport, the applied difference scheme follows with

increasing difficulties (or does not follow at all), the changes in the regions II and III caused by electrons returning from the satellite valley into the central one.

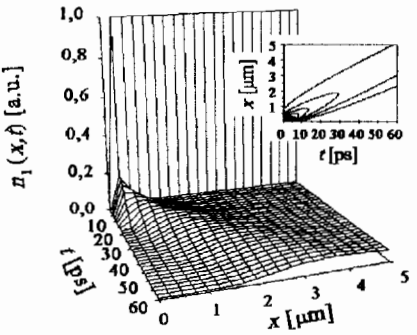

Figure 9 Spatial-temporal distribution of the normalized concentration $n_1(x,t)$ in the central (Γ) valley for the electric field intensity $E = 30\,\text{kV/cm}$

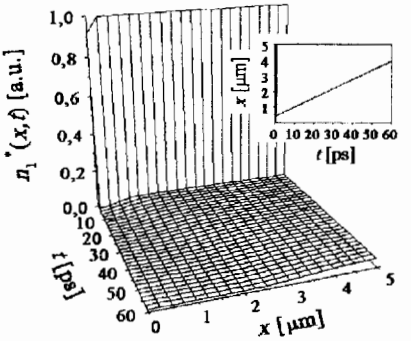

Figure 10 Spatial-temporal distribution of the normalized concentration $n_1^*(x,t)$ in the central (Γ) valley for the electric field intensity $E = 30\,\text{kV/cm}$

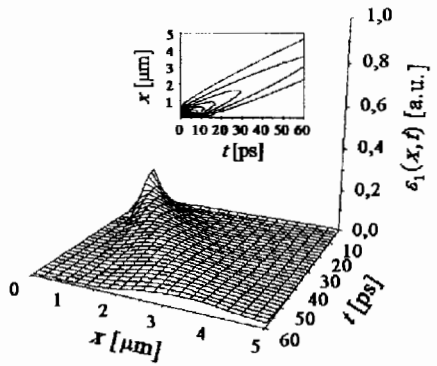

Figure 11 Spatial-temporal distribution of the difference $\varepsilon_1(x,t)$ of the obtained concentrations in the central (Γ) valley for the electric field intensity $E = 30\,\text{kV/cm}$

The return of electrons from the satellite into the central valley can be seen in the 3D figures of concentration n_1 as a "hump" spreading through the regions II and III. It can is marked for extremely strong ($E = 30\,\text{kV/cm}$) electric fields (Figure 9), while for the field of 10 kV/cm the obtained figure is the result of superposition of the spatial-temporal distributions of the carriers which are all the time transported through the central valley (region I) and the carriers returning from the satellite valleys into the central one (regions II and III).

By applying the exact solution we perceive the dynamics of the carrier transport and learn that the transport processes within the central valley proceed through two mechanisms. The primary mechanism is the flow of the carriers which practically do not leave the central valley during transport, while the other mechanism is based on the transport of carriers returned from the satellite valleys into the central valley. The second mechanism, however, cannot be perceived according to the simple numerical solution which "smoothens" the consequences of this mechanism in the diagram showing the spatial-temporal dependence of electrons within the central valley.

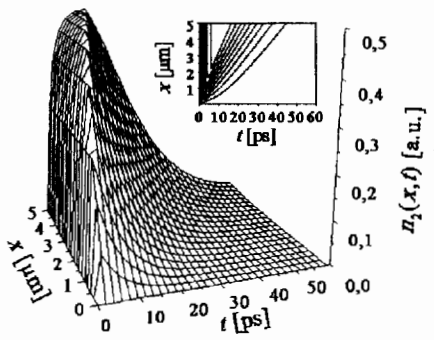

Figure 12 Spatial-temporal distribution of the normalized concentration $n_2(x,t)$ in the satellite (X, L) valleys for the electric field intensity $E = 5$ kV/cm

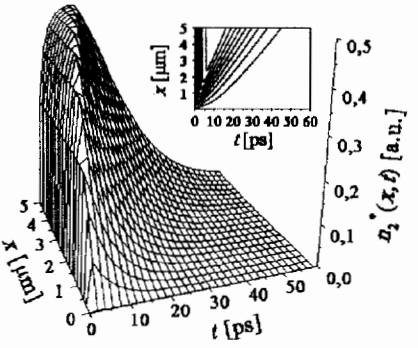

Figure 13 Spatial-temporal distribution of the normalized concentration $n_2^*(x, t)$ in the satellite (X, L) valleys for the electric field intensity $E = 5$ kV/cm

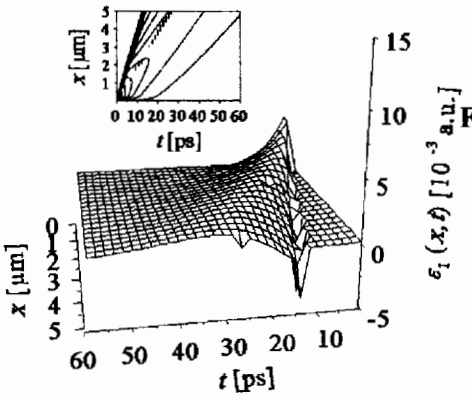

Figure 14 Spatial-temporal distribution of the difference $\varepsilon_2(x, t)$ of the obtained concentrations in the satellite (X, L) valleys for the electric field intensity $E = 5$ kV/cm

Figures 14, 17 and 20 show that the absolute discrepancy of these solutions is extremely small. Of course, the discrepancy is the largest at the beginning of the numerical procedure, the same as in the case of the central valley.

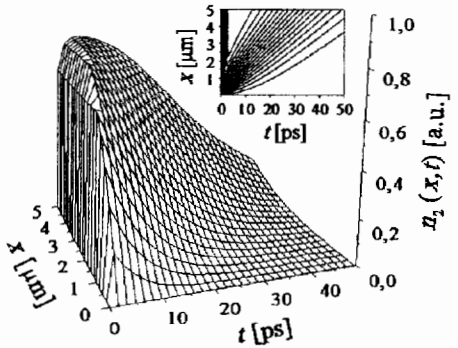

Figure 15 Spatial-temporal distribution of the normalized concentration $n_2(x,t)$ in the satellite (X, L) valleys for the electric field intensity $E = 10\,\text{kV/cm}$

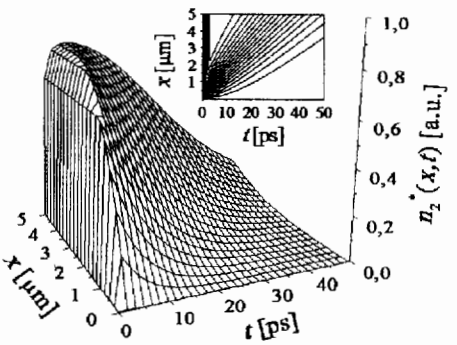

Figure 16 Spatial-temporal distribution of the normalized concentration $n_2^*(x,\ t)$ in the satellite (X, L) valleys for the electric field intensity E = 10 kV/cm

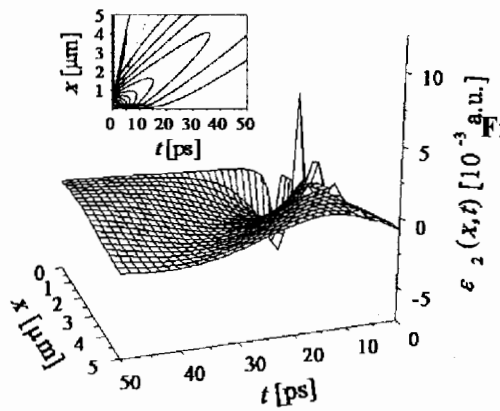

Figure 17 Spatial-temporal distribution of the difference $\varepsilon_2(x,t)$ of the obtained concentrations in the satellite (X, L) valleys for the electric field intensity $E = 10\,\text{kV/cm}$

The satellite valleys work like a "reservoir" of electrons during transport. At the initial moment it accepts the electrons from the central valley,

and then, after the number of electrons in the central valley is decreased due to transport, it returns the electrons into the central valley. In this case the numerical procedure is able to follow correctly the electron transport.

* * *

The developed analytical procedure can be applied to those two- and three-dimension-al models of semiconductor structures where the transport along one

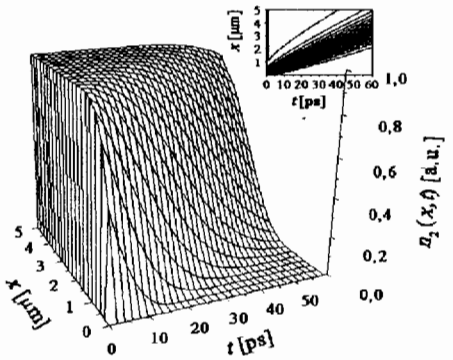

Figure 18 Spatial-temporal distribution of normalized concentration $n_2(x, t)$. The equations from in the satellite (X, L) valleys for electric field intensity $E = 30$ kV/cm

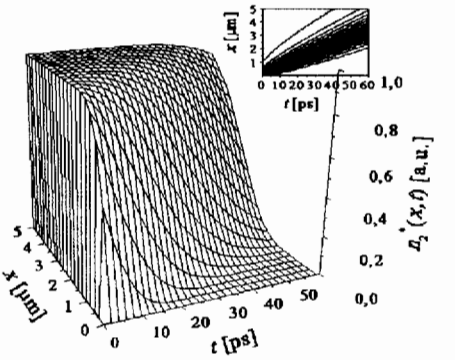

Figure 19 Spatial-temporal distribution of normalized concentration $n_2^*(x, t)$ in the satellite (X, L) valleys for electric field intensity $E = 30$ kV/cm

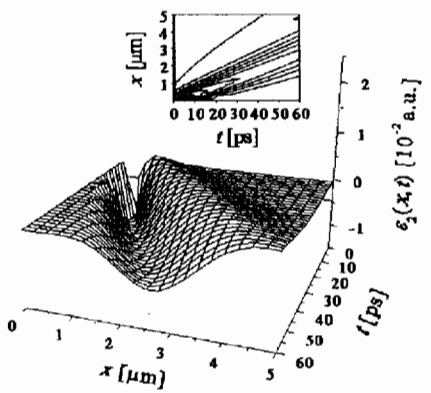

Figure 20 Spatial-temporal distribution of the difference $\varepsilon_2(x, t)$ of the obtained concentrations in the satellite (X, L) valleys for electric field intensity $E = 30$ kV/cm

of the co-ordinates may be taken as dominant in comparison to the others. Such situations occur relatively frequently (for example, see [4, 12, 14]).

This analytical technique, unfortunately, does not permit an exact tretment of multidimensional models of semiconductor structures, regardless of the other conditions, since system (1) would contain at least one more spatial variable (y and/or z) and its partial derivative. Nevertheless, for such a system it is not possible to reliably determine in advance the existence of a solution which could be represented in an analytically closed form.

Consequently, the analysis describes only the system (1). Since the transport is one-dimensional, the boundary conditions can be considered only at the contacts of the device where an electric field is established. The equations from the system (1) are practically symmetrical with regard to the partial derivatives over the variables x and t. Therefore it is justified to expect that an analytical solution could also be found in the situation where in the relation (4) at the boundary $x = 0$ DIRICHLET and NEUMANN's boundary conditions are simultaneously given, since the solution proce-dure would then be reduced to the already presented treatment of the CAUCHY problem.

The presented analytical solution could be used for qualitative and quantitative description of some other phenomena apart from the mentioned ones, depending on their character, *i.e.*, the possibility to model them, even only approximately, by equations (1), or for the different particular initial conditions of general type (4).

5. Conclusion

The work presents a detailed analysis of a general initial condition problem capable of describing the transport processes appearing in some two-valley semiconductor electron devices. A procedure is developed for one-dimensional exact explicit calculation of the function values (*i.e.*, concentrations) n_1 and n_2 for arbitrary values of the independent variables x and t, according to the expressions (17a-d), (21) and (24a-d). It is shown that a PDE system can be solved analytically (in quadratures), *i.e.*, it can be reduced to the problem of calculating of numerical values of integrals F_i and H_i, $(i = 1, 2)$, according to (18) and (25). Some of these integrals may be improper, but bearing in mind their convergence, some difficulties arising due to the singularity in the upper boundary can be easily overcome. However, in the proposed special case, describing the operation of p-i-n photodiodes, that problem disappears, and the obtained express-ions become more compact and significantly simpler for numerical calculation. The results are compared with the numerical solution obtained using the finite difference method by applying the so-called upwind scheme which is used most often for that kind of problems. A detailed analysis

is given of the obtained error, with graphical illustrations for various representative values of parameters. Apart from the de-scribed advantages, the analytical treatment offers an additional possibility to in-dependently calculate the concentrations n_1 and n_2 in an arbitrary position x and at an arbitrary moment t, while in the numerical solution there is unavoidable limitation due to the discretization of the starting problem. The numerical method also requires all the previous calculations in the discretization mesh, which significantly increases the amount of time spent on calculations when compared to the implemented analytically obtained formulae.

The accuracy of calculating of n_1 and n_2 is substantially improved in comparison with the methods of their calculation applied until now. The proposed insight into the transport mechanisms and the described physical phenomena becomes general, as opposed to the analyses known to the authors. The presented method also provides a new and very important possibility of optimization of the electric field parameter values, in order to obtain the desired optimal concentrations n_1 and n_2. Let us note at the end that, bearing in mind the accuracy of the analytical and numerical procedure, the obtained solution could serve as a kind of "standard" for assessing the efficiency of particular approximate methods for solution of the considered class of PDE systems.

Acknowledgment

The research of Iričanin B. was partly supported by The Mathematical Institute of SASA, Belgrade, Project No. 04M03.

References

[1] Blotekjaer, K. (1970) Transport equations for electrons in two-valley semiconductors *IEEE Trans. Electron Devices* **ED-17**, pp. 38-47.

[2] Courant, R., Hilbert, D. (1968) *Methoden der mathematischen Physik II* second edn (Ber-lin: Springer Verlag)

[3] Farlow, S. J. (1993) *Partial differential equations for Scientists and Engineers* second edn (New York: Dover Publications)

[4] Fatemi, E., Jerome, J., Osher, S. (1991) Solution of the Hydrodinamic Device Model Using High-Order Nonoscillatory Shock Capturing Algorithms *IEEE Trans. Compu-ter-Aided Design* **CAD-10**, 232-243.

[5] Gvozdić, D. M. (1997) Analysis of Transfer Function of Metal-Semiconductor-Metal Photodetector Equivalent Circuit *Appl. Phys. Lett.* **70**, 286-288.

[6] Hellwig, G. (1977) *Partial Differential Equations* second edn (Stuttgart: B. G. Teubner)

[7] Iričanin, B., Gvozdić, D. (1997) On the Analytic Solution for the Distribution of Electron Concentration in a Two-valley Semiconductor, in: *15th IMACS World Congress on Scien-tific Computation* ed. A. Sydow (Berlin: Wissenschaft & Technik Verlag) Vol. 3, pp.581-586.

[8] Morton, K. W. (1996) *Numerical Solution of Convection-Diffusion Problems* (London: Chapman&Hall)

[9] Press, W. H., Flannery, B. P., Teukolsky, S. A., Vetterling, W. (1986) *Numerical Recipes* (Cambridge: Cambridge University Press)

[10] Prudnikov, A. P., Brychkov, Yu. A., Marichev, O. I. (1986) *Integrals and Series, Vol. 2: Special Functions* (New York: Gordon and Breach)

[11] Radunović, J. B., Gvozdić, D. M. (1993) Nonstationary and nonlinear response of a p-i-n photodiode made of two-valley semiconductor *IEEE Trans. Electron Devices* **ED-40**, 1238-1245.

[12] Radunović, D., Radunović, J. B. (1994) Numerical simulation of two-valley semi-conductor device model based on ENO shock capturing algorithm *Int. J. Num. Modelling: El. Networks, Devices, Fields* 7, 239-252.

[13] Romberg, W. (1955) Vereinfachte numerische Integration *Det Kong. Norske Viden. Sel-skabs Forhand.* **28**, 30-36.

[14] Stenzel, R., Elschner, H., Spallek, R. (1987) Numerical simulation of GaAs MESFETs including velocity overshoot *Solid-State Electron.* **30**, 873-877.

[15] Strang, G. (1986) *Introduction to Applied Mathematics* (Wellesley: Wellesley-Cambridge Press)

[16] Walter, W. (1961) Fehlerabschätzungen bei hyperbolischen Differentialgleichungen *Arch. Rat. Mech. Anal.* 7, 249-272.

[17] Webster, A. G. (1955) *Partial differential equations of mathematical physics* second edn (New York: Dover Publications)

[18] Yoshii, A.,Tomizawa, M, (1986) New Approaches to Submicron Device Modeling, in: *Process and Device Modeling* ed. W. L. Engl (Amsterdam: North-Holland) pp. 195-227.